Inorganica Chimica Acta 516 (2021) 120166

Contents lists available at ScienceDirect

Inorganica Chimica Acta

journal homepage: www.elsevier.com/locate/ica

Research paper

Influence of substituents in 1,10-phenanthroline on the structural and photophysical properties of $W(CO)_4$(1,10-phenanthroline-type) complexes

Danilo H. Jara *, Mariano Fernández, Andrés Vega, Nancy Pizarro

Universidad Andrés Bello, Facultad de Ciencias Exactas, Departamento de Ciencias Químicas, Viña del Mar, Chile

ARTICLE INFO

Keywords:
Tungsten complexes
Photoluminescence
Lifetime
Crystal structure
Supramolecular interactions

ABSTRACT

In this work, methyl and phenyl substituents were introduced in the 2,9- and 4,7-positions of the phen ligand in order to study its impact on the structural and photophysical properties of $[W(CO)_4$(phen-type)] complexes [phen-type = 4,7-dimethyl-1,10-phenanthroline (**4,7-DMPhen**); 4,7-diphenyl-1,10-phenanthroline (**BPhen**), and 2,9-dimethyl-4,7-diphenyl-1,10-phenanthroline (**BCP**)]. Crystallographic analysis of these complexes allows to investigate the correlation between the geometrical parameters with their photophysical properties measured by steady-state and time-resolved spectroscopies. The $(OC)_{eq}$–W–$(CO)_{eq}$ angle is the most significantly influenced geometrical parameter by the substituents, showing values of 92.5°, 90.2°, and 81.2° for **$[W(CO)_4$(4,7-DMPhen)]**, **$[W(CO)_4$(BPhen)]**, and **$[W(CO)_4$(BCP)]**, respectively. The smallest angle observed for **$[W(CO)_4$(BCP)]** is attributed to a steric repulsion exerted by the methyl groups to the equatorial carbonyls. Remarkably, a smaller OC_{eq}–W–CO_{eq} angle favors the High-Energy (HE) emission band, as evidenced in the photoluminescence (PL) spectra of **$[W(CO)_4$(BCP)]**. Conversely, a greater angle favors the Low-Energy (LE) emission band, as observed in the PL spectra of **$[W(CO)_4$(4,7-DMPhen)]** and **$[W(CO)_4$(BPhen)]**. The PL lifetime of the LE emission band becomes shorter when decreasing the $(OC)_{eq}$–W–$(CO)_{eq}$ angle. Furthermore, the absorption feature was affected by the 2,9-dimethyl substituents, showing greater contribution from the high-energy shoulder on the visible absorption band. This study shows that the perturbation of the $(OC)_{eq}$–W–$(CO)_{eq}$ angle induced by the substituents in the phen ligand influences on the photophysical properties of $[W(CO)_4$(phen-type)] complexes.

1. Introduction

$[M(CO)_4(N—N)]$ complexes (M = Cr, Mo, and W; N—N = 1,10-phenanthroline or 2,2′-bipyridine derivatives), have been extensively studied since the seventies due to their broad absorption in the visible spectral region, strong negative solvatochromism effect, and unusual emission properties [1–10]. Also, it has been reported that these complexes exhibit multiple electronic transitions and two photoluminescence (PL) bands, namely high-energy (HE) and low-energy (LE) emission [2,9,10]. The origin of these bands and their emission lifetimes have been the subject of multiple research works leading, in some cases, to opposite conclusions. Specifically, discrepancies arise from the origin of the HE emission band which has been attributed to triplets of Ligand Field (^{3}LF), metal-to-ligand(CO) charge-transfer ($^3MLCT_{CO}$), and recently assigned to metal-to-ligand(N—N) charge-transfer ($^3MLCT_{N\text{-}N}$) transitions [8,10–12]. Conversely, the LE emission band has been unambiguously assigned to two lowest-lying $^3MLCT_{N\text{-}N}$ (1), and $^3MLCT_{N\text{-}N}$ (2) excited states which are in thermal equilibrium at room temperature [1,4,5,9,10]. Moreover, this class of compounds display low PL quantum yield and short excited-state lifetime, limiting their use in light-induced applications.

For this purpose, Farrel et al. studied the effects of switching the LUMO character from b_1 to a_2 symmetries in $[W(CO)_4$(phen)] and $[W(CO)_4$(tmp)] (tmp: 3,4,7,8-tetramethyl-1,10-phenanthroline) by introducing methyl substituents in the 3-,4-,7-, and 8-positions of the phen ligand [7,8]. This structural change led to a significant impact on their spectroelectrochemical properties; however, little changes were observed in their electronic and photophysical properties. Notably, a biexponential decay of the LE emission band, measured in 2-MeTHF glass at 80 K, was found for both complexes with longer lifetime for $[W(CO)_4$(tmp)]. This result suggests that a structural modification by changing substituents in the phen ligand may impact on the PL properties of $[W(CO)_4$(phen-type)] complexes (phen-type = 1,10-phenanthroline derivative). Therefore, a better understanding of the excited-

* Corresponding author.
E-mail address: q.danilohermojara@uandresbello.edu (D.H. Jara).

https://doi.org/10.1016/j.ica.2020.120166
Received 2 September 2020; Received in revised form 24 November 2020; Accepted 26 November 2020
Available online 3 December 2020

state dynamic of [M(CO)$_4$(phen-type)] complexes through the structural and electronic modification of the phen-type ligand is crucial to improve their photophysical properties for further applications.

The obtention of the crystal structure is highly desired to predict the impact of the structural modification on the optical and PL properties of one molecule. However, few reports on the crystal structure studies for [W(CO)$_4$(phen-type)] complexes have been performed, which are also essential for having precise geometrical parameters to be used in theoretical calculations [13]. To our knowledge, [W(CO)$_4$(1,10-phenanthroline)] [14] and a tetracarbonyl-tungsten with a dipyrido[3,2-a:2′,3′-c]phenazine derivative ligand [15] are the only crystallographic studies found in the Cambridge Structural Database.

In this work, we report the synthesis, structural and photophysical characterization of a series of [W(CO)$_4$(phen-type)] complexes using phen-type ligand with phenyl and methyl substituents in the 2,9- and 4,7-positions. A significant impact on the absorption and PL properties of the complexes is observed when incorporating methyl substituents in the 2 and 9 positions of the phen ligand. The results are discussed based on the crystal structure analysis of the complexes. [W(CO)$_4$(phen-type)] complexes bearing phen-type ligands with substituents in the 2- and 9-positions have not been synthesized and studied before. Hence, those new findings will be relevant to reinforce the understanding of the photophysical properties of [W(CO)$_4$(phen-type)] complexes.

2. Experimental

2.1. Materials

Tungsten hexacarbonyl 97% was purchased from Merck. 4,7-dimethyl-1,10-phenanthroline (**4,7-DMPhen**); 4,7-diphenyl-1,10-phenanthroline (bathophenanthroline, **BPhen**); 2,9-dimethyl-4,7-diphenyl-1,10-phenanthroline (Bathocuproine, **BCP**) were purchased from AK Scientific, Inc. Spectroscopic grade toluene and acetonitrile, and dried THF were purchased from Merck. All reagents and solvents were used as received.

2.2. Instrumentation

Ultraviolet–Visible (UV–Vis) absorption spectra were recorded on an Agilent Cary 8454 Diode-Array spectrophotometer using deaerated solutions at room temperature. Emission spectra were recorded in a Horiba Jobin-Yvon FluoroMax-4 spectrofluorometer at room temperature and 77 K. Photoluminescence lifetime measurements were carried out in a PicoQuant FluoTime 300 fluorescence lifetime spectrometer with a time-correlated single-photon counting technique. Picosecond laser of 375, 405, and 530 nm were employed as pulsed light sources. The NMR experiment was recorded on a Bruker Advance 400 MHz instrument using $CDCl_3$ as a solvent. The proton assignations were performed using 1D and 2D NME experiments. The solid-state structures of **[W(CO)$_4$(4,7-DMPhen)]**, **[W(CO)$_4$(Bphen)]**, and **[W(CO)$_4$(BCP)]** were determined by X-ray diffraction at room temperature using a SMART-APEX II CCD diffractometer system. Data were reduced by using SAINT(Bruker, A. P. SAINT, version 6.22; Bruker AXS Inc.: Madison, WI, 2004, DOI: https://doi.org//10.1021/jp402550g). The effect of X-rays absorption was corrected by using a multi-scan or a face-indexed approach, by using SADABS (Sheldrick, G. M. SADABS, version 2.05; Bruker AXS Inc.: Madison, WI, 2007). The structures were solved partially by using direct methods and then completed by Difference Fourier Synthesis. The structure solution and subsequent refinement by least-squares used SHELXL (Sheldrick, G. M. A short history of SHELX. Acta Crystallogr., Sect. A: Found. Crystallogr. 2008, 64, 112–122; Sheldrick, G. M. S. N. V. SHELXTL, version 6.12; Bruker AXS Inc.: Madison, WI, 2000). The positions of the hydrogen atoms were calculated after each cycle of refinement with SHELXL using a riding model, with C—H distance of 0.93 or 0.96 Å. Uiso(H) values were set equal to 1.2 or 1.5 U_{eq} of the parent carbon atom.

2.3. Synthesis of the [W(CO)$_4$(phen-type)] complexes

The synthesis for all complexes was adapted from reported procedures [16–19]. Their molecular structure is shown in Scheme 1.

2.3.1. Synthesis of [W(CO)$_4$(4,7-dimethyl-1,10-phenanthroline)], [W(CO)$_4$(4,7-DMPhen)]

0.28 mmol (100 mg) of W(CO)$_6$ were added into a one-neck round-bottom flask with 15 mL of dried THF. Then, the solution was deaerated with argon for 15 min. After degassing, the solution was irradiated for 40 min with a 365 nm led lamp. The solution changed from pale yellow to yellowish-green. A stoichiometric amount of **4,7-DMPhen** with 5% excess was dissolved in THF into a separate container and degassed with argon for 15 to 30 min. After that, the solution was carefully transferred dropwise with a syringe to the round-bottom flask. The resulting solution was irradiated for 4 h forming a dark red solution. The product was then purified on a silica chromatographic column using ethyl acetate as eluent. Yield: 116 mg (50%). ^{1}H NMR (400 MHz, $CDCl_3$) δ 9.43 (d, $J = 5.3$ Hz, H2 and H9), 8.15 (s, H5 and H6), 7.57 (d, $J = 5.3$ Hz, H3 and H8), 2.91 (s, 4-CH_3 and 7-CH_3) (See proton assignment in Fig. S1). Anal. Calcd. for $C_{18}H_{12}N_2O_4W$: C, 42.88; H, 2.40; N, 5.56; found: C, 42.69; H, 2.21; N, 5.40.

2.3.2. Synthesis of [W(CO)$_4$(4,7-diphenyl-1,10-phenanthroline)], [W(CO)$_4$(BPhen)].

The synthesis was carried out using a similar procedure than in 2.3.1. Yield: 70 mg (39%). ^{1}H NMR (400 MHz, $CDCl_3$) δ 9.64 (d, $J = 5.3$ Hz, H2 and H9), 8.03 (s, H5 and H6), 7.70 (d, $J = 5.3$ Hz, H3 and H8), 7.66–7.53 (m, 4-C_6H_5 and 7-C_6H_5) (See proton assignment in Fig. S2). Anal. Calcd for $C_{28}H_{16}N_2O_4W$: C, 53.53; H, 2.57; N, 4.46; found: C, 52.97; H, 2.40; N, 4.31.

2.3.3. Synthesis of [W(CO)$_4$(2,9-dimethyl-4,7-diphenyl-1,10-phenanthroline)], [W(CO)$_4$(BCP)]

The synthesis was carried out using a similar procedure than in 2.3.1. Yield: 163 mg (47%). ^{1}H NMR (400 MHz, $CDCl_3$) δ 7.85 (s, H3 and H8), 7.67 (s, H5, and H6), 7.61–7.48 (m, 4-C_6H_5 and 7-C_6H_5), 3.37 (s, 2-CH_3 and 9-CH_3) (See proton assignment in Fig. S3). Anal. Calcd. for $C_{30}H_{20}N_2O_4W$: C, 54.90; H, 3.07; N, 4.27; found: C, 54.60; H, 2.92; N, 4.18.

3. Results and discussion

3.1. Structural characterization

Crystals of the complexes suitable for single-crystal X-ray diffraction were obtained through liquid–liquid diffusion using acetone/hexane for **[W(CO)$_4$(4,7-DMPhen)]** and toluene/hexane for **[W(CO)$_4$(Bphen)]** and **[W(CO)$_4$(BCP)]** at room temperature. The molecular structures of each complex are depicted in Fig. 1, and selected bond lengths and angles are listed in Table 1.

Overall, the bond lengths for the three complexes exhibit only slight differences. The most significant ones are the W–N distances, being longer for **[W(CO)$_4$(BCP)]** with values of 2.262(9) and 2.273(7) Å in comparison to 2.219(2) and 2.220(2) for **[W(CO)$_4$(4,7-DMPhen)]**, and 2.225(4) and 2.229(4) for **[W(CO)$_4$(BPhen)]**.

The three complexes exhibit similar $(OC)_{ax}$–W–$(CO)_{ax}$ and N_1–W–N_2 angles with values around 170° and 73°, respectively, which are in agreement with analogous compounds [14,20,21]. The deviation of the $(OC)_{ax}$–W–$(CO)_{ax}$ angle from 180° has been attributed to the strong repulsion between the axial CO orbitals and the occupied orbitals of the phenanthroline [20]. A smaller than 90° N_1–W–N_2 angle is caused by the small bite angle of the phen ligand, which usually varies from 70° to 80°. These deviations contribute to the formation of a distorted octahedral structure observed for the [W(CO)$_4$(phen-type)] complexes. The most significant difference is the $(OC)_{eq}$–W–$(CO)_{eq}$ angle showing values of

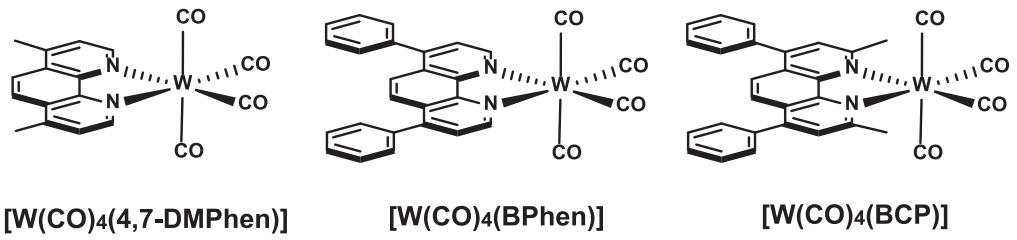

Scheme 1. Molecular structure of the [W(CO)$_4$(phen-type)] to be used in this study.

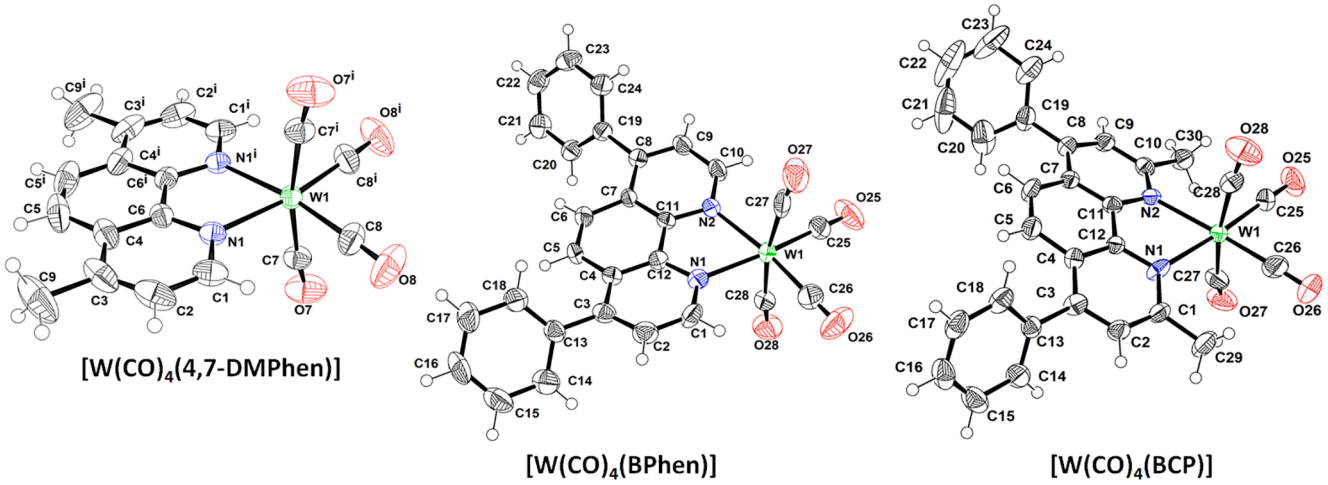

Fig. 1. ORTEP representation of the tungsten complexes with ellipsoids at 50% probability.

92.5°, 90.2°, and 81.2° for **[W(CO)$_4$(4,7-DMPhen)]**, **[W(CO)$_4$(BPhen)]**, and **[W(CO)$_4$(BCP)]**, respectively (Fig. S4). The methyl substituents in the 2- and 9-positions in **BCP** push the equatorial carbonyls due to steric repulsion decreasing the $(OC)_{eq}$–W–$(CO)_{eq}$ angle. Consequently, the angles C26–W1–N1 and C25–W1–N2 become more obtuse than in the other complexes with values of 102.0 and 104.1, respectively (Table 1).

According to the crystal structures, the phen ligands bearing phenyl substituents (**BPhen** and **BCP**) are bent from the equatorial plane (N1–W1–N2) and also exhibit a bow conformation (Fig. S1-3). These deviations are more significant when methyl groups are also included in 2- and 9-positions (**BCP**). Conversely, the ligand having only methyl substituents in the 4- and 7-positions (**4,7-DMPhen**) exhibits a planar conformation (Fig. S3). The **BPhen** and **BCP** bend in **[W(CO)$_4$(BPhen)]** and **[W(CO)$_4$(BCP)]** was quantitatively measured by the angle formed between the normal plane and a drawn line from W1 to C5/C6 atoms (Fig. S5) [22]. The obtained angles were 6° and 11° for **[W(CO)$_4$(BPhen)]** and **[W(CO)$_4$(BCP)]**, respectively. Additionally, the bow conformation adopted by **BPhen** and **BCP** ligands in their complexes was measured by the bow angle (Θ_B) with values of 12° and 19°, respectively (Fig. S6). These bent and bow conformations are attributed to steric effects exerted by the 4,7-diphenyl and 2,9-dimethyl substituents bound to the phen ligand. However, when comparing with the reported crystal structure of [Mo(CO)$_4$(neocuproine)], which has only the 2,9-dimethyl substituents, the ligand lies coplanar with its equatorial plane [13]. Therefore, we may state that 4,7-diphenyl groups are responsible for the deviation from coplanarity. Only when those substituents are present, the 2,9-dimethyls exert an additional distortion on the ligand, as detected in the crystal structure of **[W(CO)$_4$(BCP)]**. This conclusion can be applied only to octahedral complexes, supported by observing a similar conformation for the BCP ligand in Re and Os complexes' crystal structure [23,24]. Conversely, tetrahedral complexes bearing BCP ligand exhibit a planar conformation [25–28]. It is noted that few examples of crystal structures for octahedral complexes bearing BCP ligand can be found in literature, suggesting that the steric hindrance produced by phenyl groups makes the crystal packing difficult to form. Previous works have found that complexes subjected to steric hindrance avoid it by adopting deformed conformation such as twist, bow, and tilt [29,30]. This steric strain is minimized in tetracoordinate complexes by forming a tetrahedral geometry [29,31]. Deviation of planarity could also be responsible for a longer W–N bond for **[W(CO)$_4$(BCP)]** in comparison to the other complexes (Table 1).

For all complexes, the packing is stabilized by intermolecular interactions such as π-π stacking, M−CO (lone pair)···π(aryl) and hydrogen bond. Ring stacks interactions are shown in Fig. 2, and their geometrical parameters are summarized in Table 2 and Table 3. The complex **[W(CO)$_4$(4,7-DMPhen)]** exhibits an offset π-staked geometry involving two pyridine fragments of **4,7-DMPhen** with centroid–centroid distance (Cg5···Cg5^{iii}, *iii*: 2–*x*, *y*, 3/2–*z*) of 3.639 Å (Fig. 2**A**). Conversely, **[W(CO)$_4$(BPhen)]** shows π-π stacking interactions involving a phenyl groups which stacks almost face-to-face with the central aromatic ring of BPhen at Cg3···Cg1^{i} (*i*: 1 − *x*, *y* − ½, ½ − *z*) of 3.565 Å (Fig. 2**B**). An offset π-π staking is also observed between a phenyl fragment and one pyridine moiety of BPhen with Cg2···Cg3^{i} of 3.824 Å (Fig. 2**B**). Similarly, the complex **[W(CO)$_4$(BCP)]** exhibits a face-to-face π-π stacking between the same aromatic rings as in [W(CO)$_4$(Bphen)], having a Cg4···Cg1^{ii} (*ii*: 1 − *x*, *y* − ½, 1 − *z*) of 3.625 Å (Fig. 2**C**). Moreover, the complex **[W(CO)$_4$(4,7-DMPhen)]** shows a twofold M−CO_{ax} (lone pair)···π (pyridine fragment) interaction having the same distance C7–O7···Cg2 of 3.106 Å. This interaction is absent in the crystal packing of the **[W(CO)$_4$(Bphen)]** and **[W(CO)$_4$(BCP)]** complexes. However, they exhibit two primary C—H···O hydrogen bonds with distances values listed in Table 2. The M−CO (lone pair)···π(aryl) interaction has been found to contribute significantly to the crystal structure stability of metal carbonyl complexes, leading to zero- or one-dimensional aggregation patterns [32,33].

Table 1
Selected geometric parameters (Å, °) for the tungsten complexes.

[W(CO)$_4$(4,7-DMPhen)]			
W1—C8^i	1.955(3)	W1—C7	2.019(3)
W1—C8	1.955(3)	W1—N1	2.219 (2)
W1—C7^i	2.019(3)	W1—N1^i	2.220 (2)
C8^i—W1—C8	92.51(17)	C7^i—W1—N1	92.23(8)
C8^i—W1—C7^i	87.05(10)	C7—W1—N1	95.72(8)
C8—W1—C7^i	86.11(10)	C8^i—W1—N1^i	97.19(10)
C8^i—W1—C7	86.12(10)	C8—W1—N1^i	170.20(10)
C8—W1—C7	87.05(10)	C7^i—W1—N1^i	95.72(8)
C7^i—W1—C7	170.10(14)	C7—W1—N1^i	92.23(8)
C8^i—W1—N1	170.20(10)	N1—W1—N1^i	73.15(9)
C8—W1—N1	97.19(10)	C1—N1—C6	117.2(2)
[W(CO)$_4$(BPhen)]			
W1—C25	1.947(6)	W1—C27	2.022(7)
W1—C26	1.955(6)	W1—N1	2.225(4)
W1—C28	2.017(6)	W1—N2	2.229(4)
C25—W1—C26	90.2(2)	C28—W1—N1	90.25(18)
C25—W1—C28	85.2(2)	C27—W1—N1	97.25(19)
C26—W1—C28	86.1(2)	C25—W1—N2	99.38(19)
C25—W1—C27	88.3(2)	C26—W1—N2	170.22(19)
C26—W1—C27	86.5(2)	C28—W1—N2	96.60(18)
C28—W1—C27	170.1(2)	C27—W1—N2	91.75(18)
C25—W1—N1	170.48(19)	N1—W1—N2	72.84(14)
C26—W1—N1	97.8(2)		
[W(CO)$_4$(BCP)]			
W1—C26	1.94(2)	W1—C27	2.022(19)
W1—C25	1.948(10)	W1—N2	2.262(9)
W1—C28	2.018(15)	W1—N1	2.273(7)
C26—W1—C25	81.1(9)	C28—W1—N2	89.6(5)
C26—W1—C28	87.3(8)	C27—W1—N2	96.1(6)
C25—W1—C28	83.2(9)	C26—W1—N1	102.0(7)
C26—W1—C27	87.8(8)	C25—W1—N1	176.2(3)
C25—W1—C27	87.2(10)	C28—W1—N1	94.7(7)
C28—W1—C27	169.8(7)	C27—W1—N1	95.1(8)
C26—W1—N2	173.6(7)	N2—W1—N1	72.7(4)
C25—W1—N2	104.1(7)		

Symmetry code: i: $-x+1, y, -z+3/2$.

3.2. Photophysical properties

3.2.1. Electronic absorption properties

The absorption spectra of the three complexes measured in different solvents are shown in Fig. 3. A broad MLCT band is observed in the visible spectral region which exhibits a negative solvatochromism up to 100 nm when the polarity of the solvent is increased. The **[W(CO)$_4$(4,7-DMPhen)]** and **[W(CO)$_4$(BPhen)]** complexes exhibit a similar MLCT band feature, having a shoulder around 400 nm (Fig. 3**A and B**). The MLCT band of **[W(CO)$_4$(BPhen)]** is shifted to lower energy due to larger conjugation given by phenyl substituents. Remarkably, **[W(CO)$_4$(BCP)]** shows a distinct absorption pattern when compared to the typical absorption spectra of [W(CO)$_4$(phen-type)] complexes [1,4,5]. It is observed that the electronic transitions on the high-energy side (the shoulder) of the visible absorption band increase in contribution, leading to a broader MCLT band with a flat maximum. This characteristic is clearly attributed to the influence of 2,9-dimethyl substituents, which decrease the angle OC_{eq}–W–CO_{eq} affecting the energy and contribution of the orbitals involved in the electronic transition. According to Resonance Raman excitation profiles and TD-DFT calculations carried out for [W(CO)$_4$(phen)] and [W(CO)$_4$(tmp)], multiple allowed electronic transitions give rise to the visible absorption band of [W(CO)$_4$(phen-type)] complexes. The low-energy side of the absorption band is a contribution of pure W ⟶ phen-type MLCT transitions. Conversely, the high-energy side of the absorption band involves the contribution of W ⟶ Phen-type and W ⟶ CO MLCT transitions [1–3,7,8]. In general, for [W(CO)$_4$(phen-type)] complexes, theoretical calculations have shown that near 30% of the total contribution to the HOMOs corresponds to $(CO)_{eq}$ and $(CO)_{ax}$ characters. Furthermore, the W ⟶ CO MLCT transition involves a contribution of about 38% of $(CO)_{eq}$ to the HOMO and 88% of

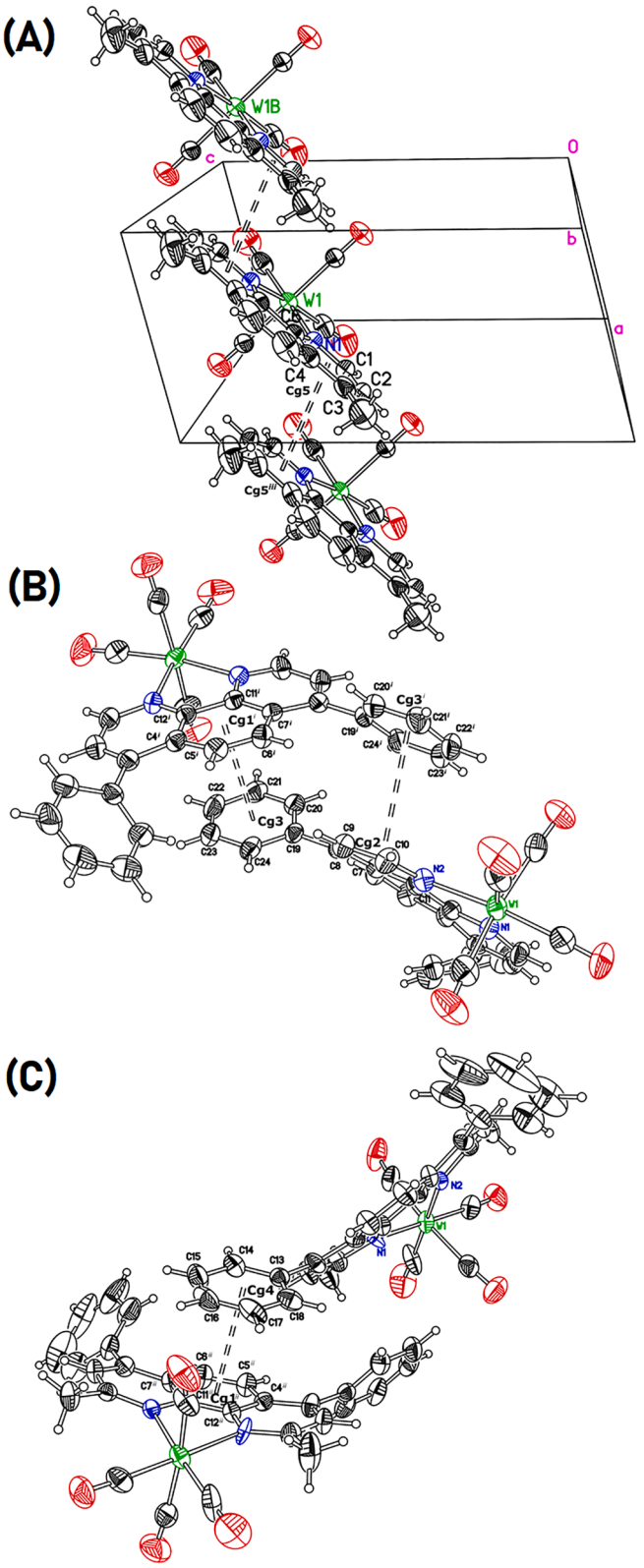

Fig. 2. ORTEP representation at 50% probability showing the π-π stacking interactions for **(A) [W(CO)$_4$(4,7-DMPhen)]**, **(B) [W(CO)$_4$(Bphen)]**, and **(C) [W(CO)$_4$(BCP)]**, (Symmetry labels: i: 1 − x, y − ½, ½ − z; ii: 1 − x, y − ½, 1 − z. iii: 2 − x, y, 3/2–z).

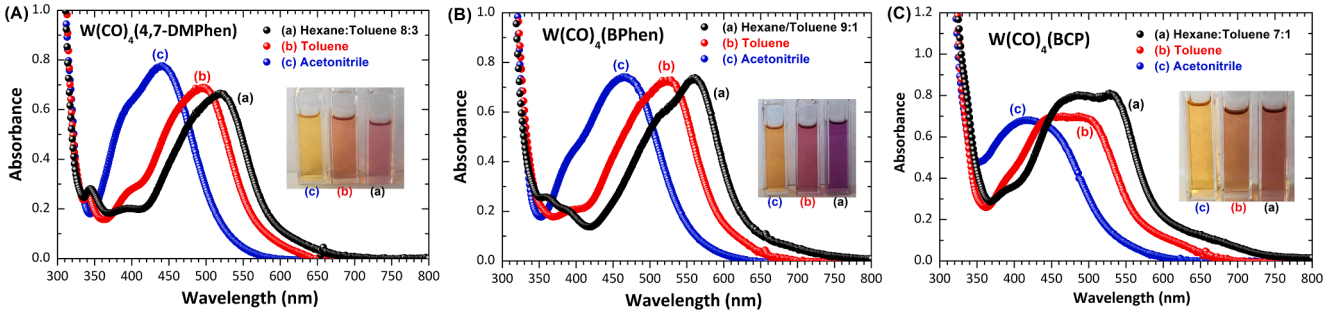

Fig. 3. Absorption spectra of the [W(CO)$_4$(phen-type)] complexes measured in solvents with different polarities. Blue line: ACN, red line: toluene and black line: hexane/toluene mixture. (For interpretation of the references to colour in this figure legend, the reader is referred to the web version of this article.)

Table 2
π-π Interaction geometry for the tungsten complexes. Centroids details: Cg1: C4, C5, C6, C7, C11 and C12; Cg2: C9, C10, C8, C7, C11 and N2; Cg3: C19, C20, C21, C22, C23 and C24; Cg4: C13 C14 C15 C16, C17 and C18; Cg5: N1, C1, C2, C3, C4 and C12.

	[W(CO)$_4$(4,7-DMPhen)]	
Interaction	ccd (Å)	ipd (Å)
Cg5···Cg5^{iii}	3.639	3.439
	[W(CO)$_4$(BPhen)]	
Cg3···Cg1^{i}	3.566	3.510
Cg2···Cg3^{i}	3.824	3.529
	[W(CO)$_4$(BCP)]	
Cg4···Cg1^{ii}	3.625	3.602

Symmetry labels: i: 1 − *x*, *y* − ½, ½ − *z*; ii: 1 − *x*, *y* − ½, 1–*z*. iii: 2 − *x*, *y*, 3/2–*z*.

Table 3
Hydrogen-bond geometry (Å) for [W(CO)4(BPhen)] and [W(CO)4(BCP)].

	[W(CO)$_4$(BPhen)]
D—H···*A*	*D*···*A*
C9—H9···O27^{iv}	3.384(7)
*C*2—H2···O26^{v}	3.211(7)
	[W(CO)$_4$(BCP)]
C29—H29*B*···O27^{vi}	3.463(18)
C9—H9···O25^{vii}	3.493(17)

Symmetry codes: iv: -*x*, *y* − ½, -*z* + ½; v: − *x*, − *y* + 1, − *z*; vi: − *x* + 1, *y* − ½, − *z* + 1; vii: − *x* + 1, *y* + ½, 2 − *z*.

(CO)$_{ax}$ to the LUMO [7]. Therefore, due to a significant CO$_{eq}$ character involved in the HOMO of [W(CO)$_4$(phen-type)] complexes, any perturbation on the OC$_{eq}$–W–CO$_{eq}$ angle may strongly influence on its energy and contribution to the electronic transitions. A change of the (CO)$_{ax}$ orbitals is excluded since the OC$_{ax}$–W–CO$_{ax}$ angle exhibits similar values for the three complexes. Previous works by Farrel et. Al. found that the absorption features of the [W(CO)$_4$(phen-type)] complexes were unaffected by switching of LUMO character between b_1 for a_2 symmetries introducing methyl groups at the 3,4,7 and 8-positions in the phen ligand [7,8]. This result is likely attributed to the lack of perturbation on the carbonyls groups. Another explanation for the change in the absorption feature for [W(CO)$_4$(BCP)] could be the electron-donating properties of methyl substituents in the 2- and 9- positions. When methyl substituents are present in these positions, changes in the photophysical properties have been observed for uncoordinated and coordinated phen-type molecules [34,35].

3.2.1.1. Steady-state photoluminescence (PL) properties at 293 K

3.2.1.1.1. Non-polar solvent (toluene). The steady-state PL properties for the three complexes were investigated using a non-polar and polar solvents at room temperature. Toluene was used as a non-polar solvent, and their PL spectra measured at various excitation wavelengths (λ_{ex}) are shown in Fig. 4. Due to the low PL intensity of the emission bands, overlapping, and near IR tail, the PL quantum yield calculation was not possible. As expected for [W(CO)$_4$(phen-type)] complexes, the low-energy (LE) emission band is observed from 650 nm to near IR region for the three compounds having a maximum wavelength around 750 to 800 nm. An emission band tail is also observed at higher energy, which corresponds to intraligand (IL) emission. In the PL spectra of **[W(CO)$_4$(BPhen)]**, using λ_{ex} from 350 to 450 nm, a low-intensity shoulder band is observed on the tail of the IL emission (Fig. 4**B**) which may correspond to the high-energy (HE) emission band. This band is also observed in the PL spectra of **[W(CO)$_4$(BCP)]** when excited from 350 to 475 nm, having a more intense and well-defined peak (Fig. 4**C**). For **[W(CO)$_4$(4,7-DMPhen)]**, the HE emission band is absent or exhibits very low PL intensity (Fig. 4**A**) which indicates that this band is not present in all [W(CO)$_4$(phen-type)] complexes as previously reported [2,4,5,15]. The dual emission band for some of these types of complexes is a peculiar characteristic, and the origin of the HE band has been the subject of various research works showing different conclusions [2,10,15].

For all complexes, excitation spectra recorded at different observed wavelengths (λ_{obs}) show that the LE band is originated from excitation on the MLCT absorption manifold (Fig. S7). Conversely, the HE emission band arises from excitation on the high-energy side of the visible absorption band, as observed in the broad excitation band (300 to 450 nm) of **[W(CO)$_4$(BPhen)]** and **[W(CO)$_4$(BCP)]** (Fig. S7 B and C). Since the HE emission band appears on the tail of the IL fluorescence, its excitation band also exhibits contribution from the IL transition.

3.2.1.1.2. Polar solvent (acetonitrile). The steady-state PL properties for the three complexes in acetonitrile (ACN) are shown in Fig. 5. Apparently, the LE emission band is weaker than recorded in toluene for **[W(CO)$_4$(4,7-DMPhen)]** and **[W(CO)$_4$(BPhen)]** (Fig. 5**A and B**), while for **[W(CO)$_4$(BCP)]** this band is almost completely quenched (Fig. 5**C**). Conversely, the HE emission band is weakly observed for **[W(CO)$_4$(4,7-DMPhen)]** and becomes more predominant for **[W(CO)$_4$(BPhen)]** and **[W(CO)$_4$(BCP)]**. In fact, for the later complex, the HE emission is the only band observed after excitation from 400 to 500 nm. This result shows that the HE emission band is not quenched by a polar solvent, as observed for the LE emission band. The excitation spectra of the HE emission band for the three complexes (Fig. S8) show an excitation band extending from 300 to 450 nm with a maximum of around 350 nm. This band confirms that the HE emission originates from the excitation on transitions contained on the high-energy side of the absorption spectra of [W(CO)$_4$(phen-type)] complexes with some contribution of the IL transition.

3.2.1.2. Steady-state PL properties at 77 K. Due to the low PL intensity of [W(CO)$_4$(phen-type)] at room temperature, steady-state experiments at 77 K in a mixture of methanol/ethanol 4:1 were conducted, and the PL spectra for the three complexes are shown in Fig. 6. Fluorescence and phosphorescence bands of the IL transitions are observed in the PL

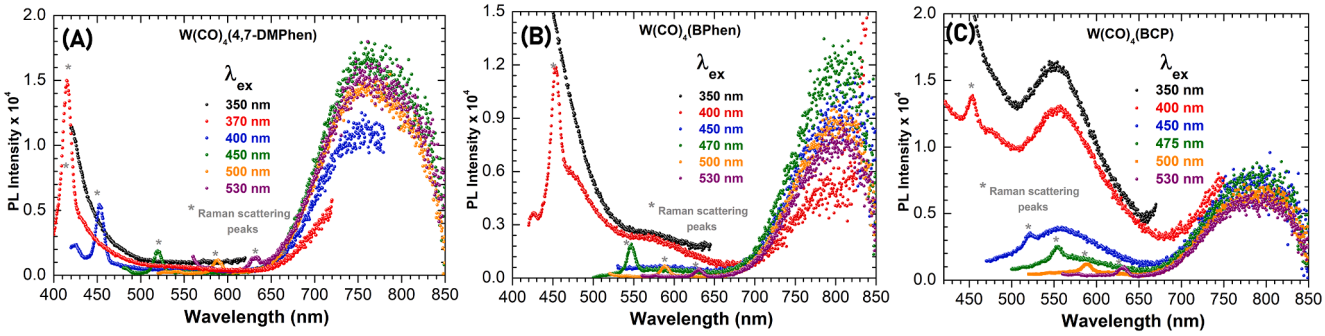

Fig. 4. PL spectra of the [W(CO)$_4$(phen-type)] complexes, measured at various excitation wavelengths (λ_{ex}) in toluene at 293 K. PL spectra are corrected for wavelength variations in detector response.

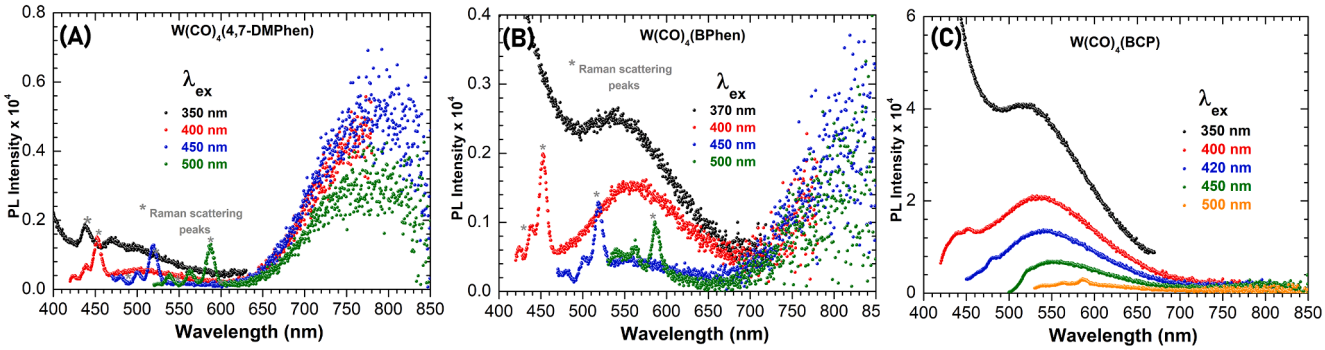

Fig. 5. PL spectra of the [W(CO)$_4$(phen-type)] complexes measured at various excitation wavelengths (λ_{ex}) in ACN at 293 K. PL spectra are corrected for wavelength variations in detector response.

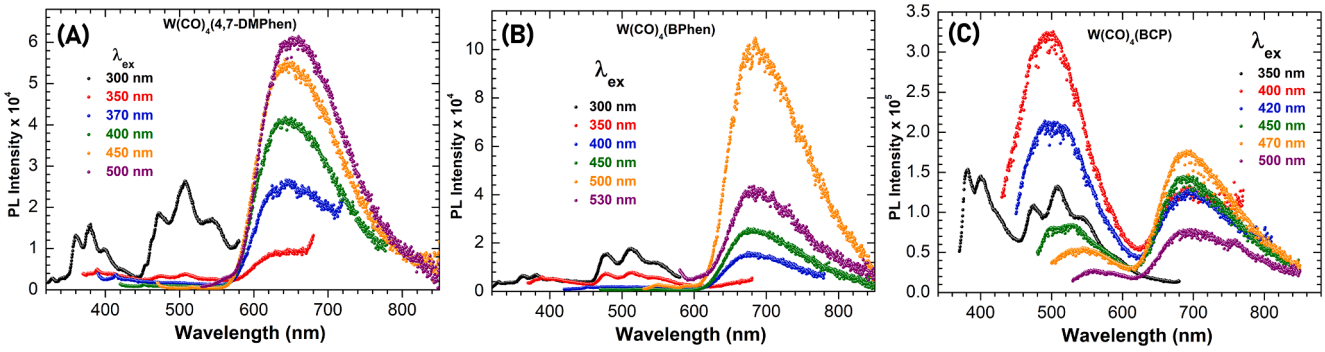

Fig. 6. PL spectra of the [W(CO)$_4$(phen-type)] complexes measured at various excitation wavelengths (λ_{ex}) in methanol/ethanol 4:1 at 77 K. PL spectra are corrected for wavelength variations in detector response.

spectra of the three complexes after excitation from 300 to 370 nm. For **[W(CO)$_4$(4,7-DMPhen)]** and **[W(CO)$_4$(BPhen)]**, the LE emission band predominates under light irradiation from 400 nm to longer wavelengths, while the HE emission band is very weak or absent (Fig. 6**A and B**). Conversely, the PL spectrum of **[W(CO)$_4$(BCP)]** shows both HE and LE emission bands at the same range of excitation wavelengths, exhibiting maxima of 495 nm and 690 nm, respectively (Fig. 6**C**). These results confirm that the 2,9-methyl substituents in BCP favor the HE emission band also at low temperatures. It is noted that the PL spectrum of **[W(CO)$_4$(BPhen)]** at 77 K does not show the HE emission band, as previously reported by Servaas et al. [3] Probably, this band was confused with the phosphorescence band from the ^{3}IL excited state since they have similar energy levels, as observed in the PL spectra of **[W(CO)$_4$(BCP)]** (Fig. 6**C**). Interestingly, the excitation band for **[W(CO)$_4$(BCP)]** monitored on the LE emission band shows two distinguished bands between 350 and 500 nm (Fig. S9C). This observation corroborates possible changes in the energy and contribution of the molecular orbitals involved in the electronic transition of **[W(CO)$_4$(BCP)]**, as observed in its absorption spectrum.

3.2.1.3. Time-resolved PL properties at room temperature (293 K) and 77 K. The PL lifetime for the three complexes at 293 K and 77 K are summarized in Table 4. The PL lifetime for the HE emission band was only detectable at 77 K for **[W(CO)$_4$(BCP)]**, because at room temperature, this band exhibits low PL intensity and is highly overlapped with the tail of the IL fluorescence band. A multiexponential decay resolved in three PL lifetimes (Table 4) was determined for this complex upon excitation at 405 nm and observed at 550 nm. We ruled out the possibility of a biexponential decay because of the elevated value of χ^2, which is not due to random error (Fig. S13-16) [36]. The shortest PL lifetimes may be attributed to the decay of the IL emission. Therefore, the HE band of **[W(CO)$_4$(BCP)]** decays with biexponential kinetics, which is in

Table 4
PL lifetimes of the $[W(CO)_4(phen\text{-}type)]$ measured at different conditions.

	τ (HE)/ns $[\lambda_{ob}]^b$, (A)[a] $\lambda_{ex} = 405$ nm	τ (LE)/ns $[\lambda_{ob}]^b$, (A)[a] $\lambda_{ex} = 530$ nm		
Temperature	77 K	293 K		77 K
Solvent	MeOH/EtOH 4:1	Toluene	ACN	MeOH/EtOH 4:1
$[W(CO)_4(4,7\text{-}DMPhen)]$	N.O.	[770 nm] 4.1	N.D.	[650 nm] (*) 167 ± 4 (70%) 524 ± 10 (27%) 3300 ± 95 (3%)
$[W(CO)_4(BPhen)]$	N.O.	[800 nm] 2.7	[800 nm] 2.6	[690 nm] 126 ± 5 (79%) 474 ± 38 (19%) 2990 ± 160 (2%)
$[W(CO)_4(BCP)]$	[500 nm] 2.0 ± 0.1 (60%) 11.0 ± 0.2 (23%) 30.0 ± 0.3 (17%)	[800 nm] 1.7	N.D.	[690 nm] (*) 12 ± 1 (42%) 70 ± 4 (38%) 268 ± 8 (20%)

(*) $\lambda_{ex} = 405$ nm.
N.O. = No observed in the PL spectrum.
N.D. = No detected.
[a] Fractional amplitude.
[b] Observed wavelength.

agreement with other $[W(CO)_4(phen\text{-}type)]$ complexes [5,8]. Conversely, at 293 K a monoexponential kinetics was determined for the LE emission band decay, with PL lifetime values decreasing in the order of **$[W(CO)_4(4,7\text{-}DMPhen)]$** > **$[W(CO)_4(BPhen)]$** > **$[W(CO)_4(BCP)]$**. This tendency implies that attaching methyl substituents in the 2- and 9-positions of the phen ligand increases the non-radiative rate constant from the LE emissive excited state, ^{3}MLCT(phen). At low temperature, the LE emission decay showed a significant lengthening of the PL lifetimes in comparison to room temperature due to rigidochromic effect, which is in agreement with previous works [5,7,8]. However, the decay was found to be resolved using a tri-exponential kinetic rather than a bi-exponential one (higher value of χ^2). Therefore, our results demonstrate that the LE emission band comprises three ^{3}MLCT(phen-type) excited states rather than two, as previously proposed [5,8,10], which are in thermal equilibrium at room temperature but unequilibrated at 77 K. Nevertheless, three low-lying ^{3}MLCT(phen-type) excited states are supported by theoretical calculations and Resonance Raman excitation profiles where these triplet excited states have been evidenced [3,8].

3.3. *Overview of the structural influence on the photophysical properties of the $[W(CO)_4(phen\text{-}type)]$ complexes*

In the PL spectra of $[W(CO)_4(phen\text{-}type)]$ complexes at room temperature, an emission band tail is observed in the higher energy side of the HE emission band after excitation below 400 nm. Most of the previous studies on this type of complexes have shown PL spectra from 500 nm to lower energy, preventing a careful analysis of the UV–Vis region. Farrell, I.R. et al. speculated that this emission might be attributed to solvent impurities, scattered laser light, or solvent Raman scattering; however, no experimental evidence was shown [8]. Conversely, we ascribe this emission band tail to originate from the IL excited state of the coordinated phen-type ligand. Fig. S17 shows that the free ligands' emission band tail can extend toward 550 to 600 nm after excitation at 350 nm. The absence of free ligand in the ^{1}H NMR spectra for all complexes rules out the possibility that this emission comes from uncoordinated phen-type ligand. Furthermore, simultaneous emission from both ligand and MLCT excited states have been previously reported for Re and Cu complexes, supporting our assignment [37,38].

As discussed, the incorporation of 2,9-dimethyl substituents in the phen ligand has a strong influence on the photophysical properties of the $[W(CO)_4(phen\text{-}type)]$ complexes. To support this finding, we also synthesized and carried out a photophysical analysis of **$[W(CO)_4(2,9\text{-}DMPhen)]$**, where **2,9-DMPhen** = 2,9-dimethyl-1,10-phenanthroline. For this complex, similar absorption features and PL properties to **$[W(CO)_4(BCP)]$** were observed (Fig. S5-7 and Table S1). This fact corroborates that the 2,9-dimethyl substituents are the main responsible for the differences in the photophysical properties of the complexes when they are compared to analogous complexes without these substituents. This experimental evidence may be ascribed to a steric constraint of methyl groups imposed over the equatorial carbonyls in the plane, resulting in a more acute $(OC)_{eq}$–W–$(CO)_{eq}$ angle, as evidenced by the crystal structure analysis. Consequently, a second steric repulsion is produced between the equatorial carbonyls, leading to a change in the energy of their molecular orbitals and the contribution to the electronic transitions where these orbitals participate. A more significant contribution from the high-energy side of the visible absorption band was observed for **$[W(CO)_4(BCP)]$** as a consequence of a smaller $(OC)_{eq}$–W–$(CO)_{eq}$ angle. This observation suggests the involvement of a W ⟶ CO MLCT transition on this side of the absorption spectrum for $[W(CO)_4(phen\text{-}type)]$ complexes, supporting previous conclusions on this assignment [7–9,11,12].

The steric repulsion produced by 2,9-dimethyl substituents also affects the PL properties of the tungsten complexes. Our results indicate that HE emission band is not always present in $[W(CO)_4(phen\text{-}type)]$ complexes as observed in the PL spectra of **$[W(CO)_4(4,7\text{-}DMPhen)]$** and **$[W(CO)_4(BPhen)]$** in toluene and at low temperature (Figs. 4 and 6); however, in ACN, this band weakly appears. Conversely, for **$[W(CO)_4(BCP)]$** and **$[W(CO)_4(2,9\text{-}DMPhen)]$** having 2,9-dimethyl substituents in the phen ligand, the HE emission band was favored in all conditions, while the LE emission band is almost completely quenched in ACN. A similar PL behavior has been observed for Cu(I) complexes based on phen ligands, where the ^{3}MLCT emission band is quenched when measured in coordinating solvents such as ACN due to an exciplex formation [39,40]. A similar process might also explain the quenching of the LE emission band in the ACN solution for $[W(CO)_4(phen\text{-}type)]$ complexes. This hypothesis is supported by the fact that the photosubstitution mechanism for $[W(CO)_4(phen\text{-}type)]$ complexes are predominantly associative under visible light irradiation [6,9]. However, if the exciplex formation takes place, the relaxation of the excited state should decay by a different pathway, and the HE emission should also be quenched.

Another explanation is ascribed to a change in the relative energy order positions of the ^{1}MLCTs and ^{3}MLCTs excited states as a consequence of a structural change and solvatochromic effect (Scheme 2). Firstly, we state that the excited state energy of the ^{1}MLCT(phen) is lying below the ^{3}MLCT(CO) excited state. After excitation on the high-energy side of the visible absorption band (400–450 nm), the ^{1}MLCT(CO) excited state is populated and rapidly relaxes to the ^{1}MLCT(phen), and ^{3}MLCT(CO) excited states. Then, the ^{3}MLCT(phen) excited state is predominantly populated by these two states and decays via radiative deactivation to the ground state; in contrast, the ^{3}MLCT(CO) relaxes mainly via non-radiative decay. This mechanism is illustrated in Scheme 2**A** and would explain the PL properties observed for **$[W(CO)_4(4,7\text{-}DMPhen)]$** and **$[W(CO)_4(BPhen)]$** in toluene, and at low temperature, where the LE emission is the only band observed (Figs. 4 and 6). A second case (Scheme 2**B**) occurs when the ^{1}MLCT(phen) excited state rises in energy due to the solvatochromism effect lying slightly over the ^{3}MLCT(CO) excited state. Conversely, the ^{1}MLCT(CO) transition energy is weakly affected by the polarity of the solvent. This change in energy now allows the ^{1}MLCT(phen) excited state to be deactivated through the ^{3}MLCT(phen) and ^{3}MLCT(CO) excited states.

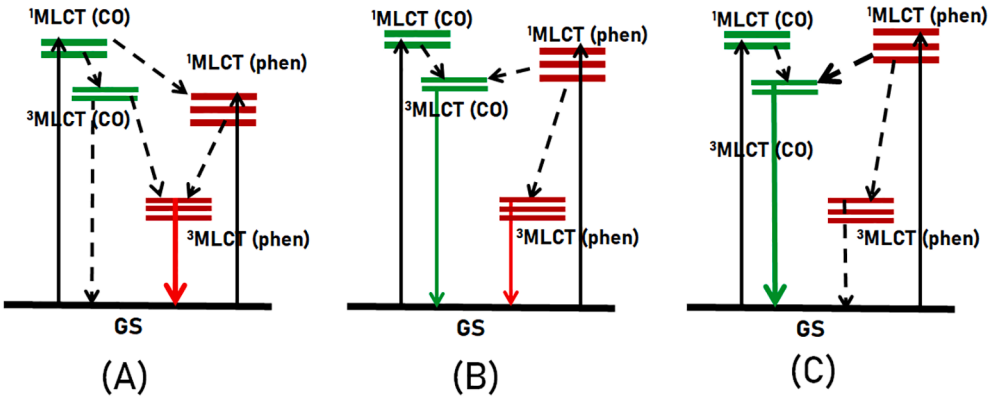

Scheme 2. Excited-state deactivation mechanism explaining the PL behavior for the $[W(CO)_4$(phen-type)] complexes. The diagram shows only the primary excited state levels involved in the deactivation and the prominent non-radiative decay. Bold arrows indicate the primary process involved in the excited state deactivation.

The latter having enough population to relax through radiative decay. This mechanism is depicted in Scheme 2**B**. In this case, the HE emission band is weakly observed, and the LE emission band decreases in intensity, as shown in the PL spectra of **[W(CO)$_4$(4,7-DMPhen)]** and **[W(CO)$_4$(BPhen)]** in ACN. A similar mechanism would explain the PL properties of **[W(CO)$_4$(BCP)]** and **[W(CO)$_4$(2,9-DMPhen)]** in toluene, where both HE and LE emission band are observed. However, in absolute terms, the HE emission band is more emissive than the LE band; hence, the 2,9-dimethyl substituents in the phen ligand may increase the radiative rate constant from ^{3}MLCT(CO) to the ground state. Finally, a third mechanism, illustrated in Scheme 2**C**, would explain the PL properties of **[W(CO)$_4$(BCP)]** and **[W(CO)$_4$(2,9-DMPhen)]** in ACN. Here, the ^{1}MLCT(phen) excited state rises more in energy due to structural influence and solvent effect, lying above the ^{3}MLCT(CO) excited state. Consequently, ^{1}MLCT(phen) excited state deactivates efficiently to ^{3}MLCT(CO) state which relaxes to the ground state via radiative decay. Therefore, LE emission is quenched, and the HE emission is the only band observed in the PL spectra of **[W(CO)$_4$(BCP)]** and **[W(CO)$_4$(2,9-DMPhen)]** measured in ACN, as observed in Fig. 3.

4. Conclusions

In conclusion, we have demonstrated that the incorporation of methyl and phenyl substituents in different positions of the phen ligand has an impact on the structural and photophysical properties of $[W(CO)_4$(phen-type)] complexes. Crystal structure analysis of **[W(CO)$_4$(4,7-DMPhen)]**, **[W(CO)$_4$(Bphen)]**, and **[W(CO)$_4$(BCP)]** showed a bent of the phen ligand from the equatorial plane and a bow conformation when phenyl groups are attached to the 4- and 7-positions. Furthermore, the crystal packing revealed that these complexes are stabilized by π-π, M−CO (lone pair)···π(aryl) and hydrogen bond interactions. Remarkably, methyl substituents in the 2- and 9-positions impact substantially on the $(OC)_{eq}$–W–$(CO)_{eq}$ angle exhibiting values of 92.5°, 90.2°, and 81.2° for **[W(CO)$_4$(4,7-DMPhen)]**, **[W(CO)$_4$(Bphen)]**, and **[W(CO)$_4$(BCP)]**, respectively. As a consequence, a change in the absorption feature and a higher contribution of the HE emission band was observed for **[W(CO)$_4$(BCP)]**. The 2,9-dimethyl substituents in the phen ligand exert a steric effect on the equatorial carbonyls changing their orbital energy and contribution to the electronic transitions of the complex. This fact was confirmed by the preparation and photophysical analysis of **[W(CO)$_4$(2,9-DMPhen)]**, which exhibits similar properties to **[W(CO)$_4$(BCP)]**. For **[W(CO)$_4$(4,7-DMPhen)]** and **[W(CO)$_4$(BPhen)]**, the LE emission band is predominant, and no evidence of the HE emission band was found in toluene at 293 K and in MeOH/EtOH at 77 K, contrary to previous reports. Furthermore, the LE emission band was partially quenched for **[W(CO)$_4$(4,7-DMPhen)]** and **[W(CO)$_4$(Bphen)]**, and completely quenched for **[W(CO)$_4$(BCP)]** in ACN. The PL lifetime of LE emission band measured in toluene at 293 K for the three complexes displays a single exponential time decreasing in the order of **[W(CO)$_4$(4,7-DMPhen)]** > **[W(CO)$_4$(BPhen)]** > **[W(CO)$_4$(BCP)]**. Therefore, to extend the PL lifetime of the LE emission for $[W(CO)_4$(phen-type)] complexes, no substitution at the 2- and 9-positions should be attached, while the HE emission band is favored when introducing substituents in those positions. The PL behavior of these complexes was explained based on a change in the position of the excited state energy levels due to structural and solvatochromism effect. In summary, we have demonstrated that the perturbation on the $(OC)_{eq}$–W–$(CO)_{eq}$ angle by substituents in the 2- and 9-positions of the phen ligand dictates the favoring of the HE and LE emission band in the PL spectrum of $[W(CO)_4$(phen-type)] complexes.

CRediT authorship contribution statement

Danilo H. Jara: Conceptualization, Methodology, Investigation, Writing - original draft, Visualization, Funding acquisition, Project administration. **Mariano Fernández:** Investigation. **Andrés Vega:** Investigation, Visualization. **Nancy Pizarro:** Resources.

Declaration of Competing Interest

The authors declare that they have no known competing financial interests or personal relationships that could have appeared to influence the work reported in this paper.

Acknowledgments

D.H.J. would like to thank to postdoctoral FONDECYT grant 3180327. N.P. acknowledges partial financial support from FONDECYT-Chile (Grant 1160749) and CONICYT FONDEQUIP (EQM160099). A.V. acknowledges Financiamiento Basal Proyecto FB0807 (CEDENNA) for financial support.

Appendix A. Supplementary data

Supplementary data associated with this article can be found in the online version. CCDC 1987994, 1987995 and 1987996 contains the crystallographic data and can be obtained free of charge from the Cambridge Crystallographic Data Centre, 12 Union Road, Cambridge CB2 1EZ, UK; fax: (+44) 1223-336-033; or e-mail: deposit@ccdc.cam.ac.uk. Supplementary data to this article can be found online at https://doi.org/10.1016/j.ica.2020.120166.

References

[1] M. Wrighton, D.L. Morse, J. Organomet. Chem. 96 (1975) 998–1003, https://doi.org/10.1021/ja00811a008.

[2] D.M. Manuta, A.J. Lees, Inorg. Chem. 22 (1983) 572–573, https://doi.org/10.1021/ic00145a046.
[3] P.C. Servaas, H.K. Van Dijk, T.L. Snoeck, D.J. Stufkens, A. Oskam, Inorg. Chem. 24 (1985) 4494–4498, https://doi.org/10.1021/ic00220a015.
[4] D.M. Manuta, A.J. Lees, Inorg. Chem. 25 (1986) 1354–1359, https://doi.org/10.1021/ic00229a012.
[5] K.A. Rawlins, A.J. Lees, Inorg. Chem. 28 (1989) 2154–2160, https://doi.org/10.1021/ic00310a028.
[6] R. van Fu, Eldik, Inorg. Chem. 37 (1998) 1044–1050, https://doi.org/10.1021/ic9707366.
[7] I.R. Farrell, F. Hartl, S. Záliš, T. Mahabiersing, J.A. Vlček, J. Chem. Soc., Dalton Trans. (2000) 4323–4331, https://doi.org/10.1039/b005279p.
[8] I.R. Farrell, J. van Slageren, S. Zalis, A. Vlcek, Inorg. Chim. Acta 315 (2001) 44–52, https://doi.org/10.1016/S0020-1693(01)00308-5.
[9] A. Vlcek, Coord. Chem. Rev. 230 (2002) 225–242, https://doi.org/10.1016/S0010-8545(02)00047-4.
[10] M. Rohrs, D. Escudero, J. Phys. Chem. Lett. 10 (2019) 5798–5804, https://doi.org/10.1021/acs.jpclett.9b02477.
[11] S. Zalis, M. Busby, T. Kotrba, P. Matousek, M. Towrie, A. Vlcek Jr., Inorg. Chem. 43 (2004) 1723–1734, https://doi.org/10.1021/ic035089z.
[12] S. Zalis, I.R. Farrell, A. Vlcek Jr., J. Am. Chem. Soc. 125 (2003) 4580–4592, https://doi.org/10.1021/ja021022j.
[13] G.A. Ardizzoia, M. Bea, S. Brenna, B. Therrien, Eur. J. Inorg. Chem. 2016 (2016) 3829–3837, https://doi.org/10.1002/ejic.201600647.
[14] Q. Ye, Q. Wu, H. Zhao, Y.-M. Song, X. Xue, R.-G. Xiong, S.-M. Pang, G.-H. Lee, J. Organomet. Chem. 690 (2005) 286–290, https://doi.org/10.1016/j.jorganchem.2004.09.020.
[15] X. Cui, J.J. Hoff, J.D. Ji, T. Albers, J. Zhao, W. He, L. Zhu, S. Miao, Inorg. Chim. Acta 442 (2016) 145–150, https://doi.org/10.1016/j.ica.2015.11.032.
[16] A.J. Lees, A.W. Adamson, J. Am. Chem. Soc. 104 (1982) 3804–3812, https://doi.org/10.1021/ja00378a005.
[17] J.P. Bullock, C.-Y. Lee, B. Hagan, H. Madhani, J. Ulrich, Aust. J. Chem. 70 (2017) 1006–1015, https://doi.org/10.1071/CH17256.
[18] H. Frisell, B. Aakermark, Organometallics 14 (1995) 561–563, https://doi.org/10.1021/om00001a078.
[19] R.J. Kazlauskas, M.S. Wrighton, J. Am. Chem. Soc. 104 (1982) 5784–5786, https://doi.org/10.1021/ja00385a039.
[20] I. Veroni, C. Makedonas, A. Rontoyianni, C.A. Mitsopoulou, J. Organomet. Chem. 691 (2006) 267–281, https://doi.org/10.1016/j.jorganchem.2005.07.023.
[21] A.O. Youssef, M.M.H. Khalil, R.M. Ramadan, A.A. Soliman, Transition Met. Chem. 28 (2003) 331–335, https://doi.org/10.1023/a:1022987521974.
[22] D. Havrylyuk, D.K. Heidary, L. Nease, S. Parkin, E.C. Glazer, Eur. J. Inorg. Chem. 2017 (2017) 1687–1694, https://doi.org/10.1002/ejic.201601450.
[23] D.K. Orsa, G.K. Haynes, S.K. Pramanik, M.O. Iwunze, G.E. Greco, D.M. Ho, J. A. Krause, D.A. Hill, R.J. Williams, S.K. Mandal, Inorg. Chem. Commun. 11 (2008) 1054–1056, https://doi.org/10.1016/j.inoche.2008.05.033.
[24] Y.-Y. Choi, W.-T. Wong, J. Organomet. Chem. 573 (1999) 189–201, https://doi.org/10.1016/S0022-328X(98)00705-0.
[25] F.K. Klemens, P.E. Fanwick, J.K. Bibler, D.R. McMillin, Inorg. Chem. 28 (1989) 3076–3079, https://doi.org/10.1021/ic00314a043.
[26] L. Smolko, J. Černák, M. Dušek, J. Titiš, R. Boča, New J. Chem. 40 (2016) 6593–6598, https://doi.org/10.1039/C6NJ00372A.
[27] A.A. Titov, O.A. Filippov, A.F. Smol'yakov, A.A. Averin, E.S. Shubina, Dalton Trans. 48 (2019) 8410–8417, https://doi.org/10.1039/C9DT01355E.
[28] R.J. Butcher, E. Sinn, Inorg. Chem. 16 (2002) 2334–2343, https://doi.org/10.1021/ic50175a037.
[29] A. Hazell, O. Simonsen, O. Wernberg, Acta Cryst. C 42 (1986) 1707–1711, https://doi.org/10.1107/S0108270186090844.
[30] S.E. Denmark, J.A. Siegel, Topics in Stereochemistry, Volume 25, Wiley, 2006.
[31] S. Geremia, L. Randaccio, G. Mestroni, B. Milani, J. Chem. Soc., Dalton Trans. (1992) 2117–2118, https://doi.org/10.1039/DT9920002117.
[32] J. Zukerman-Schpector, I. Haiduc, E.R.T. Tiekink, Adv. Organomet. Chem. 60 (2012) 49–92, https://doi.org/10.1016/B978-0-12-396970-5.00002-5.
[33] J. Zukerman-Schpector, I. Haiduc, E.R.T. Tiekink, Chem. Commun. 47 (2011) 12682–12684, https://doi.org/10.1039/c1cc15579b.
[34] G. Accorsi, A. Listorti, K. Yoosaf, N. Armaroli, Chem. Soc. Rev. 38 (2009) 1690–1700, https://doi.org/10.1039/b806408n.
[35] C.O. Dietrichbuchecker, P.A. Marnot, J.P. Sauvage, J.R. Kirchhoff, D.R. Mcmillin, J. Chem. Soc., Chem. Commun. (1983) 513–515, https://doi.org/10.1039/C39830000513.
[36] J.R. Lakowicz, Principles of Fluorescence Spectroscopy, 3rd ed., Springer, US, 2006.
[37] S.M. Fredericks, J.C. Luong, M.S. Wrighton, J. Am. Chem. Soc. 101 (1979) 7415–7417, https://doi.org/10.1021/ja00518a054.
[38] L. Lemus, J. Guerrero, J. Costamagna, R. Lorca, D.H. Jara, G. Ferraudi, A. Oliver, A. G. Lappin, Dalton Trans. 42 (2013) 11426–11435, https://doi.org/10.1039/C7DT02244A.
[39] M.W. Blaskie, D.R. Mcmillin, Inorg. Chem. 19 (1980) 3519–3522, https://doi.org/10.1021/ic50213a062.
[40] D.R. Mcmillin, J.R. Kirchhoff, K.V. Goodwin, Coord. Chem. Rev. 64 (1985) 83–92, https://doi.org/10.1016/0010-8545(85)80043-6.